Free Carrier Generation in Semiconductors Induced by Absorption of Subband-Gap Light

D. Vanmaekelbergh and L. van Pieterson

Debye Institute, University of Utrecht, P.O. Box 80000, 3508 TA Utrecht, The Netherlands

(Received 9 May 1997)

The mechanisms of electron-hole pair generation in a semiconductor induced by absorption of a subband-gap photon and mediated by a band-gap state are reviewed. The steady-state photocurrent quantum yield and the photocurrent response to harmonic modulation of the light intensity are calculated for each mechanism. It is shown, with a nanoporous GaP photoanode as an example, that the mechanisms can be distinguished by intensity-modulated photocurrent spectroscopy and that characterization of the mediating band-gap states is possible. [S0031-9007(97)05033-3]

PACS numbers: 73.50.Gr, 73.20.–r, 73.40.Mr

The generation of free carriers in a semiconducting crystal by direct or phonon assisted absorption of photons with energy larger than the band gap has been studied extensively and interpreted on a fundamental basis [1]. Less attention has been paid to absorption of photons of energy considerably (at least several kT) smaller than the band gap. Absorption of subband-gap photons is strongly enhanced by the presence of localized electronic states in the band gap. In (pure) single crystalline solids, the absorption of subband-gap photons is therefore very weak. Amorphous semiconductors have a considerable density of localized states with energy in the gap giving rise to absorption of subband-gap photons. Crystalline nanostructured and nanoporous semiconductors and insulators exhibit a huge volume density of surface atoms [2]. The optoelectric properties of such systems are strongly influenced by the interaction of photons with surface-localized electrons. For example, strong scattering and absorption of subband-gap photons have been observed in such systems [3,4]. It is of fundamental interest to understand the interaction of light with surface-localized electrons in a nanostructured system.

Single subband-gap optical transitions in a semiconductor or insulator lead to *one type* of free carrier (free holes *or* free electrons). Several techniques, such as optical absorption spectroscopy, transient photoconductivity, and surface photovoltage spectroscopy are used to explore single subband-gap optical transitions to characterize band-gap states localized in the bulk or at the surface of the semiconductor [5–8]. In addition, it has been observed that with semiconductor devices showing diode characteristics, illumination with subband-gap light may result in a steady-state photocurrent [3,4,9–11]. This implies that a subband-gap optical transition leads to a free electron *and* hole. Hence, a subband-gap optical transition, which generates a free carrier of one type, must be accompanied by another process (optical, thermal) which leads to a free carrier of the other type. In this Letter, the main mechanisms of electron-hole pair generation induced by subband-gap photon absorption are reviewed. The photocurrent quantum yield according to each mechanism is calculated. It is shown that the mechanisms can be distinguished on the basis of the photocurrent response due to a harmonically modulated intensity of subband-gap light. The potential of intensity-modulated photocurrent spectroscopy, with subband-gap light, for the characterization of band-gap states is illustrated with results obtained with nanoporous GaP photoanodes. It is shown that, due to the coupling of an optical and a thermal process in the generation of a free electron and hole, the mediating band-gap states can be probed with an energy resolution of the order of k_BT. This is, in principle, a much higher resolution than can be achieved with methods based on the optical generation of only one type of carrier.

We consider a semiconductor which is deviced in such a way that there is a region (of width L) in which photogenerated electron-hole pairs are effectively separated. Usually, this retrieval layer extends from the contact between the semiconductor and another phase (metal, electrolyte) to a depth L in the semiconductor. The absorption depth of subband-gap light is much larger than L, which makes that the spatial dependence of the light intensity $\Phi(x)$ can be neglected [$\Phi(x = 0) = \Phi(x = L)$, further denoted as Φ]. In Figs. 1(a)–1(d), the mechanisms of electron-hole pair generation induced by absorption of a subband-gap photon are sketched. There are three different mechanisms 1(a), 1(b), and 1(c) and a variation on mechanism 1(b), which involves interfacial band-gap states only. The mechanisms are shown for an *n*-type semiconductor. It is assumed that the localized states are distributed in energy over the band gap, the density of localized states is denoted as $s(E)$. In mechanism 1(a), a valence band electron absorbs a photon of energy $h\nu$ and is promoted to an empty localized state at energy E in the band gap. The rate of this process per band-gap state at E is given by the optical transition probability between $E - h\nu$ and E times the density of valence band states at $E - h\nu$ times the light intensity Φ [5]. The rate will further be denoted as $k(E - h\nu, E)\Phi$. The hole generated at $E - h\nu$ relaxes very fast to the top of the valence band. The electron in the band-gap state at E can be thermally excited into a delocalized state at the bottom of the conduction band with a rate $\varepsilon(E, E_c)$ equal to $\beta_n N_c \exp[(E - E_c)/k_BT]$, β_n being the rate constant for the capture of a conduction band electron in a band-gap

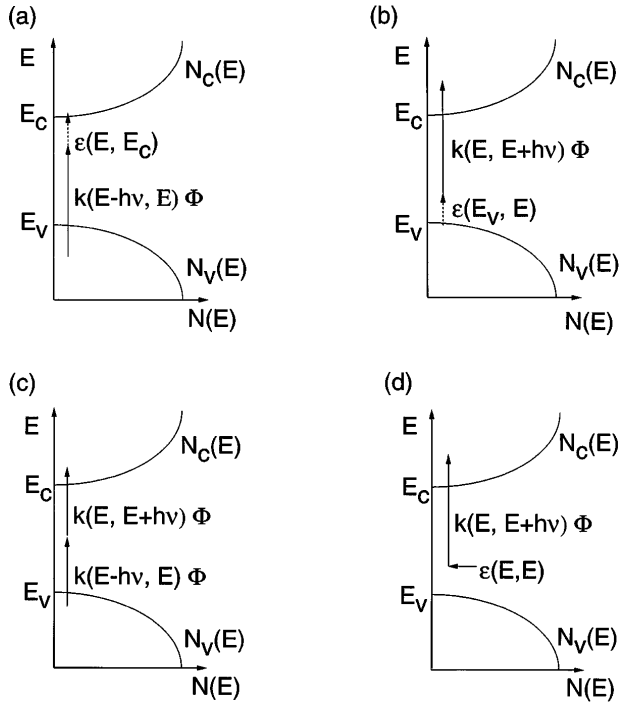

FIG. 1. (a)–(d) Mechanisms of electron-hole pair generation induced by absorption of a subband-gap photon, mediated by localized band-gap states. The vertical arrows indicate optical and thermal electron transitions, respectively. In (d), states are filled due to interfacial electron transfer (horizontal arrow).

state and N_c the effective density of states at the bottom of the conduction band [12]. It will be assumed that the band-gap states are characterized by one value of β_n. As a result of the two processes of mechanism 1(a), an electron at the bottom of the conduction band and a hole at the top of the valence band is generated. If these processes occur in the retrieval layer of the semiconductor, a steady-state photocurrent due to absorption of subband-gap light can be measured in the external circuit. In mechanism 1(b), an electron from a localized state in the band gap at energy E is optically excited into a conduction band state at $E + h\nu$. The rate per band-gap state is denoted as $k(E, E + h\nu)\Phi$. The empty state in the band gap can be filled by thermal excitation of an electron from the top of the valence band, with a rate denoted as $\varepsilon(E_\nu, E)$ given by a formula similar to that for $\varepsilon(E, E_c)$ [12]. In mechanism 1(c), an electron-hole pair is generated by consecutive absorption of two subband-gap photons (rates denoted as $k(E - h\nu, E)\Phi$ and $k(E, E + h\nu)\Phi$, respectively). Finally, mechanism 1(d) may also contribute to the photocurrent. This mechanism is mediated by *interfacial* band-gap states only. Absorption of a photon by an electron in an interfacial band-gap state results in a free majority carrier (here an electron in an *n*-type semiconductor) and an empty interfacial state, which is filled by isoenergetic transfer [rate $\varepsilon(E, E)$] of an electron from the adjacent phase (metal or electrolyte).

The electron occupation factor of the band-gap states, $f(E, t)$, according to mechanism 1(a) is determined by

$$df(E,t)/dt = k(E - h\nu, E)\Phi(t)[1 - f(E,t)] - \varepsilon(E, E_c)f(E,t)\,. \quad (1)$$

The concentration of electrons in the conduction band, n, generated by mechanism 1(a) follows from

$$dn(t)/dt = \int_{E_v}^{E_c} s(E)\varepsilon(E, E_c)f(E,t)\,dE - dj_n(t)/dx\,. \quad (2)$$

In Eq. (2), the first term on the right-hand side is the optical-thermal generation rate of electrons in the conduction band according to mechanism 1(a), and $j_n(t)$ is the flux of electrons in the retrieval region nearby the rectifying contact. The steady-state subband-gap photocurrent density, i, corresponding to mechanism 1(a) is then given by

$$i = e\int_0^L dj_n = L\int_{E_v}^{E_c} s(E)\varepsilon(E, E_c)f(E)\,dE\,, \quad (3)$$

in which the electron occupation factor $f(E)$ under steady-state conditions is given by $k(E - h\nu, E)\Phi/[k(E - h\nu, E)\Phi + \varepsilon(E, E_c)]$. The subband-gap photocurrent quantum yield according to process 1(a) can be written as

$$i/e\Phi = L\int_{E_v}^{E_c} [i(E)/e\Phi]\,dE\,, \quad (4)$$

in which $i(E)/e\Phi$ is the contribution (in $\mathrm{eV}^{-1}\,\mathrm{cm}^{-1}$) of localized states in the band gap at energy E given by $s(E)[k(E - h\nu, E) + \varepsilon(E, E_c)/\Phi]f(E)[1 - f(E)]$. In intensity-modulated photocurrent spectroscopy (IMPS), a harmonically modulated light intensity, $\Phi(\omega)$, varying with a frequency ω and having a small amplitude, is superimposed on the background light intensity Φ. The harmonically varying photocurrent density response, $i(\omega)$, is measured in the external circuit. The optoelectrical admittance is defined as $i(\omega)/e\,\Phi(\omega)$. With subband-gap illumination of energy $h\nu$, the optoelectrical admittance might be complex due to the limited rate by which the second charge carrier is (thermally) released after the optical transition. The optoelectrical admittance according to process 1(a) is calculated from Eqs. (1) and (2):

$$i(\omega)/e\Phi(\omega) = L\int_{E_v}^{E_c} [i(E)/e\Phi]\chi(\omega, E)\,dE\,, \quad (5)$$

in which the complex function $\chi(\omega, E)$ is given by

$$\chi(\omega, E) = \varepsilon(E, E_c)/[\sqrt{-1}\omega + k(E - h\nu, E)\Phi + \varepsilon(E, E_c)]\,. \quad (6)$$

It should be noted that the low frequency limit of $[i(E)/e\Phi]\chi(\omega, E)$ equals the derivative $di(E)/ed\Phi$.

In the following, it will be assumed that the probability of the optical transition of a valence band electron at $E - h\nu$ to a band-gap state at E does not depend strongly on E. The rate of optical filling of the band-gap states, $k(E - h\nu, E)\,\Phi$, will gradually decrease with increasing

E, due to a decrease in the density of valence band states with increasing $E - h\nu$ towards the top of the valence band. Since we exclude optical transitions between band-gap states $k(E - h\nu, E)$ is zero in the energy range above $E = E_v + h\nu$. The rate $\varepsilon(E, E_c)$ of the thermal transition of an electron from a state at energy E to the bottom of the conduction band increases exponentially with increasing E. Therefore, the function $f(E)[1 - f(E)]$ shows a sharp peak around the energy at which it holds that $k[E - h\nu, E]\Phi = \varepsilon(E, E_c)$. At sufficiently high light intensities, the maximum in $f(E)[1 - f(E)]$ is found close to $E = E_v + h\nu$. It then follows that the photocurrent quantum yield and the optoelectrical admittance are dominated by states in a small energy region (width $4k_BT$) around $E = E_v + h\nu$:

$$i/e\Phi = L\,(k_BT)\,s(E = E_v + h\nu)\,k(E_v, E_v + h\nu)\,, \qquad (7)$$

$$i(\omega)/e\Phi(\omega) = [i/e\Phi]\,\chi(\omega, E = E_v + h\nu)\,. \qquad (8)$$

From Eqs. (6)–(8), it follows that a plot of the optoelectrical admittance according to mechanism 1(a) in the complex plane is a semicircle in the (Re = positive, Im = negative) quadrant. The low frequency limit is a value on the real axis equal to half of the steady-state subband-gap photocurrent quantum yield. The high frequency limit is zero. The characteristic frequency, ω_a, of the semicircle is given by $2\varepsilon(E = E_v + h\nu, E_c)$ equal to $2\beta_n N_c \exp[(E_v - E_c + h\nu)/k_BT]$.

The results for the other mechanisms are summarized in Table I which displays $i(E)/e\Phi$ for the steady state and $\chi(\omega, E)$ for the optoelectrical admittance which is determined by $[i(E)/e\Phi]\chi(\omega, E)$. From the table, it follows that for each mechanism, the contribution of band-gap states at energy E to the steady-state photocurrent quantum yield and the optoelectrical admittance is proportional to the product $f(E)[1 - f(E)]$. However, only for the cases 1(a) and 1(b), in which one of the charge carriers is thermally excited from a band-gap state to a delocalized state, $f(E)[1 - f(E)]$ may show a sharp maximum as a function of E. In the case of mechanism 1(c) (consecutive absorption of two photons), it is expected that $f(E)[1 - f(E)]$ shows a relatively broad peak with a maximum around midgap if the photon energy exceeds half of the band-gap energy. Furthermore, it is clear that the four mechanisms can be distinguished on the basis of the optoelectrical admittance [see $\chi(\omega, E)$]. In the case of mechanism 1(a), a semicircle in the (Re = positive, Im = negative) quadrant is found, between half of the steady-state quantum yield at sufficiently low frequency and zero at high frequency. In the case of mechanism 1(b), a semicircle in the (Re = positive, Im = negative) quadrant is found, between half of the steady-state quantum yield at low frequency and the steady-state quantum yield at high frequency.

The potential of IMPS for investigation of the mechanism of free carrier generation induced by absorption of subband-gap light will be illustrated with results obtained with nanoporous single crystalline *n*-GaP photoanodes (band gap = 2.25 eV) illuminated with light from a He-Ne laser ($h\nu = 1.96$ eV). It will also be shown that characterization of the mediating band-gap states is possible. A single crystalline network, consisting of interconnected structural units in the 100 nm range, can be prepared on single crystalline *n*-type GaP by anodic etching under dielectric breakdown conditions [3]. It was shown that electron-hole pairs, generated with supraband-gap light, are separated with 100% efficiency in such a network [3]. In addition, it was shown that nanoporous GaP photoanodes exhibit a reasonable steady-state photocurrent

TABLE I. The contribution $i(E)/e\Phi$ to the photocurrent quantum yield for states with a density $s(E)$ in the band gap, and the complex function $\chi(\omega, E)$ determining the optoelectrical admittance, according to the main mechanisms of free carrier generation with subband-gap light. In mechanism 1(d), the energy dependence of the isoenergetic transfer rate $\varepsilon(E, E)$ depends strongly on the nature of the process. No general predictions can be made for the energy dependence of $f(E)[1 - f(E)]$ in this case. The photocurrent quantum yield corresponding to processes 1(a) and 1(b) should increase with increasing temperature, due to the fact that one of the charge carriers is thermally released from a band-gap state into the conduction or valence band, respectively. This is in contrast with the photocurrent quantum yield for mechanism 1(c).

Mechanism	$i(E)/e\Phi$	$\chi(\omega, E)$
(a)	$s(E)[k(E - h\nu, E) + \varepsilon(E, E_c)/\Phi] \times f(E)[1 - f(E)]$	$\dfrac{\varepsilon(E, E_c)}{\sqrt{-1}\,\omega + k(E - h\nu, E)\Phi + \varepsilon(E, E_c)}$
(b)	$s(E)[k(E, E + h\nu) + \varepsilon(E_v, E)/\Phi] \times f(E)[1 - f(E)]$	$\dfrac{\sqrt{-1}\,\omega + \varepsilon(E_v, E)}{\sqrt{-1}\,\omega + k(E, E + h\nu)\Phi + \varepsilon(E_v, E)}$
(c)	$s(E)[k(E - h\nu, E) + k(E, E + h\nu)] \times f(E)[1 - f(E)]$	1
(d)	$s(E)[k(E, E + h\nu) + \varepsilon(E, E)/\Phi] \times f(E)[1 - f(E)]$	$\dfrac{\sqrt{-1}\,\omega + \varepsilon(E, E)}{\sqrt{-1}\,\omega + k(E, E + h\nu)\Phi + \varepsilon(E, E)}$

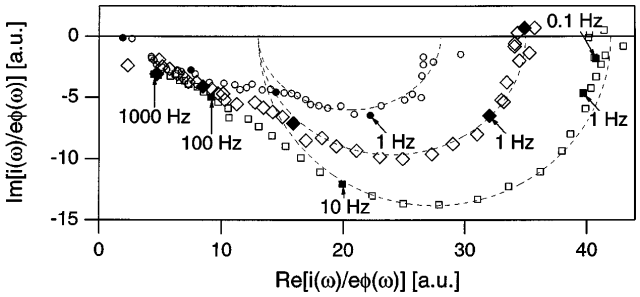

FIG. 2. Complex plane plot of the optoelectrical admittance with the modulation frequency ω as a parameter. The measurements were performed with a nanoporous *n*-GaP photoanode (thickness is 50 μm) in aqueous electrolyte, with intensity-modulated He-Ne laser light ($h\nu = 1.96$ eV) at three different temperatures. (∘) 275 K, (◇) 303 K, and (□) 322 K.

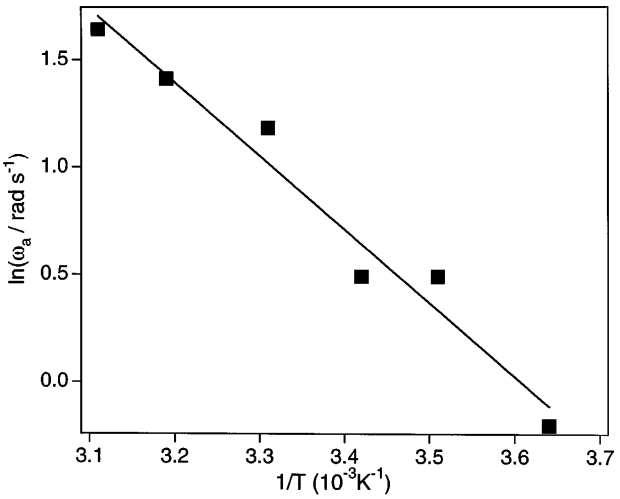

FIG. 3. Plot of the characteristic frequency ω_a of the semicircle observed in the lower frequency region as $\ln(\omega_a/\mathrm{rad}\,s^{-1})$ vs $1/T$. From the slope, an activation energy of 0.3 eV is found.

quantum yield for 1.96 eV subband-gap light (in the 10^{-4}–10^{-2} range), which increases proportional to the thickness of the porous layer [4]. In Fig. 2, a typical plot of the optoelectrical admittance in the complex plane is given, with ω as a parameter. Two semicircles are observed. The diameter of the semicircle in the lower frequency range increases with temperature; the diameter of the higher frequency loop is independent of temperature. The two loops indicate that the subband-gap photocurrent is due to two phenomena. Since the semicircle in the lower frequency region is found in the (Re = positive, Im = negative) quadrant and reflects a temperature dependent phenomenon, mechanism 1(a) must be involved. This was further checked by plotting the characteristic frequency of the semicircle as $\ln(\omega_a/s^{-1})$ vs $1/T$ (see Fig. 3). A linear relationship is found with an activation energy of 0.3 eV ± 0.05 eV. This value corresponds to the activation energy for thermal excitation of an electron from $E_v + 1.96$ eV into the conduction band as predicted for mechanism 1(a). It can be concluded that optical excitation of electrons from delocalized states near the top of the valence band to localized states as $E_v + h\nu$, followed by thermal excitation of the electrons into the conduction band, is a dominant mechanism for free carrier generation in GaP photoanodes. From extrapolation of the plot to $1/T = 0$, a value of 10^{-19}–10^{-20} cm^2 is determined for the cross section (= β_n/thermal velocity) for electron capture by the localized states. Furthermore, it was observed that the diameter of the low frequency loop markedly increases if H_2O_2 was added to the electrolyte. H_2O_2 chemisorbs on the GaP surface [4] and increases in this way the density of interfacial band-gap states involved in mechanism 1(a). It is hence proved that the band-gap states involved in mechanism 1(a) are located at the GaP/electrolyte interface. The semicircle observed at higher frequencies is not affected by H_2O_2 addition. The diameter is independent of light intensity and of temperature. This indicates that part of the free carriers is generated by consecutive absorption of two photons, mediated by localized bulk states. The frequency dispersion in the higher frequency range reflects diffusive transport of photogenerated electrons through the nanostructured GaP network [13,14].

[1] J. I. Pankove, *Optical Processes in Semiconductors* (Prentice-Hall, Inc., Englewood Cliffs, 1971).

[2] If we assume that a nanostructured nanoporous semiconductor consists of closest-packed spheres of radius *r*, the volume density of surface atoms can be estimated from $0.73\,\{[4\pi r^2]/[(4/3)\pi r^3]\}[10^{15}\ \mathrm{cm}^{-2}]$. For systems consisting of spheres with radius of 100, 10, and 1 nm, the volume density of surface atoms is then $0.5\ 10^{20}$ cm^{-3}, $0.5\ 10^{21}$ cm^{-3}, and $0.5\ 10^{22}$ cm^{-3}, respectively. For comparison, the density of GaAs units in single crystalline GaAs is about 10^{22} cm^{-3}.

[3] B. H. Erné, D. Vanmaekelbergh, and J. J. Kelly, Adv. Mater. **7**, 739 (1995).

[4] F. Iranzo Marín, M. A. Hamstra, and D. Vanmaekelbergh, J. Electrochem. Soc. **143**, 1137 (1996).

[5] G. Chiarotti, G. Del Signore, and S. Nannarone, Phys. Rev. Lett. **21**, 1170 (1968).

[6] J. Lagowski, Surf. Sci. **299/300**, 92 (1994).

[7] A. O. Evwaraye, S. R. Smith, and W. C. Mitchel, J. Appl. Phys. **77**, 4477 (1995).

[8] N. G. Semaltianos, G. Karczewski, B. Hu, T. Wojtowicz, and J. K. Furdyna, Phys. Rev. B **51**, 17 499 (1995).

[9] K. H. Beckmann and R. Memming, J. Electrochem. Soc. **116**, 368 (1969).

[10] J.-N. Chazalviel, M. Stefenel, and T. B. Truong, Surf. Sci. **134**, 865 (1983).

[11] G. Nogami, S. Okhubo, L. Avalle, and K. Hongo, J. Electrochem. Soc. **143**, 3600 (1996).

[12] J. G. Simmons and G. W. Taylor, Phys. Rev. B **4**, 502 (1971).

[13] D. Vanmaekelbergh, F. Iranzo Marín, and J. van de Lagemaat, Ber. Bunsen-Ges. Phys. Chem. **100**, 616 (1996).

[14] P. E. de Jongh and D. Vanmaekelbergh, Phys. Rev. Lett. **77**, 3427 (1996).